# PLASTIC DEFORMATION AND MICROHARDNESS OF $Pb_{1-x}Yb_xTe$ SINGLE CRYSTALS UNDER QUASI-STATIC AND SCLEROMETRIC INDENTATION

DARIA GRABCO[1], VALENTINA NICORICI[2], DARIA TOPAL[1,2], CONSTANTIN PYRTSAC[1], OLGA SHIKIMAKA[1]

[1] Institute of Applied Physics, MD-2028 Chisinau, Republic of Moldova
[2] State University of Moldova, MD-2009 Chisinau, Republic of Moldova
*E-mail:* grabco@mail.ru

*Received June 28, 2021*

*Abstract.* In this work, the microhardness and specificity of deformation of $Pb_{1-x}Yb_xTe$ single crystals by quasi-static and sclerometric indentation are studied. It is shown that these crystals are distinguished by high plasticity and low microhardness both under indentation and under the movement of the indenter. An opinion is expressed that the mechanism of crystal structure compaction is involved in mass transfer during the formation of an imprint, along with the dislocation mechanism. Crystals have low sclerometric anisotropy of hardness along different crystallographic directions on the (001) plane, which is typical for crystals of a cubic system. The jump-like mechanism of the deformation process during the movement of the indenter, which is characteristic of crystals of different types, is confirmed.

*Key words*: $Pb_{1-x}Yb_xTe$ single crystals, quasi-static and sclerometric microindentation, hardness, anisotropy, jump-like deformation mechanism during indenter motion.

## 1. INTRODUCTION

Binary compounds of lead chalcogenides, in particular PbTe, are extensively used in semiconductor instrumentation technology. Ternary compounds obtained by lead telluride doping with Group III elements (In, Ga), give rise to shallow and deep impurity levels in the charge carriers energy spectrum and, thereby, make it possible to effectively control the electrophysical, optical, photoelectric and other properties of this compound [1–3]. Doping of PbTe with ytterbium is known to result in anomalously long lifetimes of nonequilibrium charge carriers and a high photosensitivity of the doped crystals. In $Pb_{1-x}Yb_xTe$ alloys, the deep ytterbium level can vary depending on the alloy composition, being located both in the forbidden band and in the valence band, near its top. It was found that in PbTe and $Pb_{1-x}Yb_xTe$ alloys, ytterbium can be located relative to the lead sublattice both in the neutral $Yb^{2+}$ and in the $Yb^{3+}$ charged state [4, 5]. The exceptional electrophysical properties of lead chalcogenides allow them to be widely used as the main elements of sensitive IR-photodetectors, in thermoelectric devices, lasers and strain gauges and can significantly increase the capabilities of devices based on them [5].

However, unlike the electrophysical properties, which are thoroughly studied, the plastic and strength properties of these compounds are yet poorly examined, although a perfect microstructure and qualitative mechanical characteristics are a prerequisite for the long-term and reliable operation of modern microelectronic devices. Therefore, this work is a continuation of previous works [6–8] for the purpose of a more detailed study of the micromechanical properties of lead telluride doped with the rare earth element ytterbium.

Crystals of lead chalcogenides belong to the class of narrow-gap semiconductors. Thus, the band gap of PbTe is 0.32 eV, and its electrophysical properties strongly depend on the degree of deviation from stoichiometry: with an excess of lead atoms, the crystals have *n*-type conductivity, whereas those with an excess of chalcogenides have *p*-type conductivity. PbTe is crystallized in a cubic structure of the NaCl type, and the bonds between atoms are ionic-covalent. According to the data in [9], the microhardness of pure PbTe is 0.698 GPa, which is typical for compounds containing lead [10].

As was established in [8], the $Pb_{1-x}Yb_xTe$ crystals with different contents of ytterbium in the charge mixture ($x$ = 0.0025, 0.0075, and 0.01 at.%) in a wide range of loads ($P$ = 50–1000 mN) showed pronounced plasticity and low values of microhardness ($H$ = 0.35–0.39 GPa), which is noticeably lower than that of pure PbTe.

In this work, the task is to continue studying the effect of the ytterbium content on the strength, plastic, and anisotropic properties of $Pb_{1-x}Yb_xTe$ crystals in a wider range of ytterbium concentrations ($x$ = 0.004 – 0.279 wt. %).

## 2. MATERIALS AND METHODS

To solve the problem, $Pb_{1-x}Yb_xTe$ crystals were grown from the melt using the vertical Bridgman method. The ratio of the components in the charge mixture for the crystal growth corresponded to the ytterbium content with $x$ = 0.0025 (Yb content = 0.25 at.%). The synthesis was carried out for 24 hours in a container, which was later used for the crystal growing [11].

Taking into account that, when growing from a melt, the composition of the solid solution can deviate from that of stoichiometric, the resulting ingot was cut perpendicular to the growth axis sequentially along the crystal into plate-disks of about 1.5 mm thick. The ingot was divided into 14 sections along its length, and the following 6 sections were selected from them: 2, 4, 6, 11, 13, and 14. The determination of the ytterbium content in the selected samples was carried out by the X-ray fluorescence on a Cross Roads Scientific XRS-FP instrument. Table 1 shows the elemental composition of the samples.

Based on Table 1 data, we can say that the Yb content in the initial section of the ingot is significantly higher than that in the rest of its part, which indicates the value of the segregation coefficient $k > 1$. Thus, in the process of growing, Yb is

pulled out of the melt into the solid phase more in the beginning of crystallization, and in the rest of the ingot its content becomes inhomogeneous and is much less than its content in the charge.

*Table 1*

XRS-FP Analysis of set of $Pb_{1-x}Yb_xTe$ crystals from a single ingot 99B02/

| Element | Weight % of elements in the $Pb_{1-x}Yb_xTe$ 99B02/… crystals *(in brackets under each value is the measurement error on the XRS-FP device)* | | | | | |
|---|---|---|---|---|---|---|
| | 99B02/**2** | 99B02/**4** | 99B02/**6** | 99B02/**11** | 99B02/**13** | 99B02/**14** |
| **Pb** | 40.944 *(0.454)* | 41.636 *(0.297)* | 42.129 *(0.262)* | 42.131 *(0.264)* | 41.442 *(0.377)* | 42.821 *(0.292)* |
| **Yb** | 0.279 *(0.117)* | 0.032 *(0.047)* | 0.073 *(0.034)* | 0.004 *(0.029)* | 0.042 *(0.090)* | 0.011 *(0.043)* |
| **Te** | 58.777 *(1.921)* | 58.332 *(1.181)* | 57.798 *(1.059)* | 57.864 *(1.056)* | 58.516 *(1.554)* | 57.168 *(1.165)* |
| Total | 100 | 100 | 100 | 100 | 100 | 100 |

The microstructure of the surface of the samples and the relief of the zone of hardness imprints were investigated by optical microscopy on XJL-101 and Amplival devices with digital monitoring, on an MII-4 microinterferometer and by the AFM method using an Nanostation device. The study of microhardness was carried out by the quasi-static microindentation and sclerometry methods on a PMT-3 microhardness tester with a Vickers indenter at three loads ($P$ = 50, 200, and 500 mN) for microindentation and at one load $P$ =100 mN for microscratching. To obtain a more objective information on the deformation specificity 10 imprints (indentations) were applied at each load. Quasi-static microhardness was calculated as the arithmetic mean, using the following formula [12, 13]:

$$H = 1854P/d^2 \tag{1}$$

where $P$ is the load on the indenter; and $d$ is the diagonal of the Vickers imprint.

Microscratching was performed using the "edge forward" Vickers indenter. Accordingly, the microscratch hardness ($H_s$) was calculated using the following formula:

$$H_s = 1854P/b^2, \tag{2}$$

where $P$ is the load on the indenter; and $b$ is the width of the scratch.

To study the hardness anisotropy, scratches were applied along different directions from 0 to 180º every 15º, 5 scratches along each direction. After measuring the width of the scratches and determining the sclerometric hardness, a hardness rosette was plotted.

## 3. RESULTS AND DISCUSSION

### 3.1. MICROSTRUCTURE AND QUASI-STATIC TESTS OF $Pb_{1-x}Yb_xTe$ CRYSTALS

Figure 1 shows the microstructure of the surface of two samples, number 2 and number 14, from the beginning of the ingot and close to its end. It can be seen that the surface of both chips is fairly smooth, on which small defects of various types are visible, dark dots ranging in size from 1 to 2–3 microns, elongated formations of several microns, as well as longer filamentous defects of the order of ten or more microns. These defects are located on the surface of the crystals randomly, with approximately the same density on both samples.

The images in Fig. 1 also demonstrate imprints made at different loads: a, c – at a load of 50 mN; b, e and c, f, respectively, at loads of 200 and 500 mN. For better clearness, in the upper left corner of the images, the imprints are shown at a higher magnification. All imprints demonstrate high plasticity.

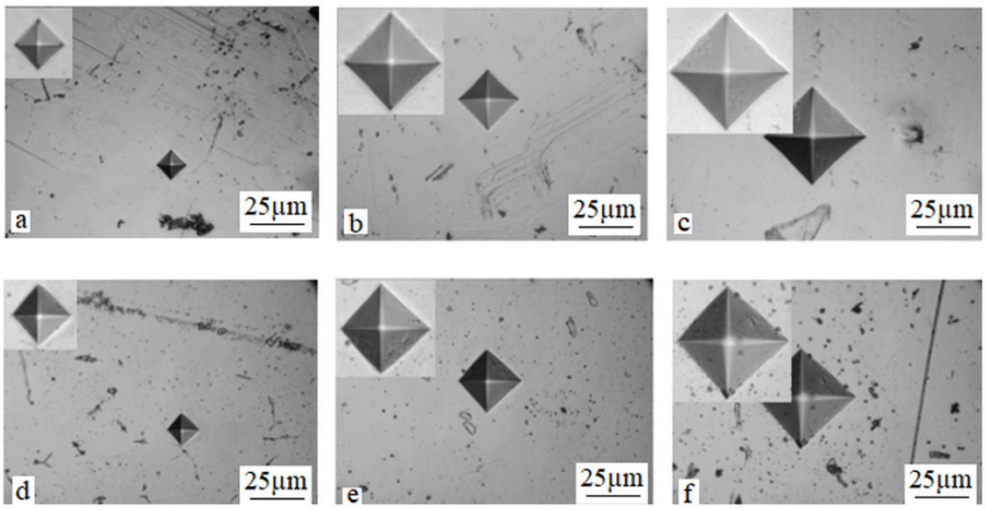



Fig. 1 – Surface microstructure on $Pb_{1-x}Yb_xTe$ samples with different Yb concentrations and image of imprints applied with loads of $P$ = 50, 200 and 500 mN. (a–c) – sample nr. 2; (d–f) – sample nr. 14. Top left corner shows imprints at higher magnification.

It should be noted that under all loads, the imprints have an almost square shape, with hardly noticeable local concavity or convexity of the sides, which indicates weak anisotropic properties of imprints. To confirm the aforementioned, the surface relief near the imprint in the interference mode (Fig. 2) and in the atomic force microscopy mode (Fig. 3) is shown as an example.

It can be seen from the figure that a very small pile-up exists near one side of the imprint and there are almost no sink-ins or other displaced material around the imprint (Fig. 2). The effect is seen even more clearly in AFM mode (Fig. 3). So, the pile-ups make up an insignificant proportion in comparison with the size of the imprint. It indicates the participation of the mechanism of compaction of the structure during plastic deformation, along with the usual dislocation mechanism of mass transfer during the imprint formation. This conclusion also agrees with the results obtained earlier in [8].

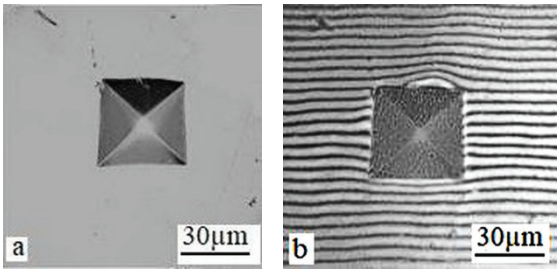
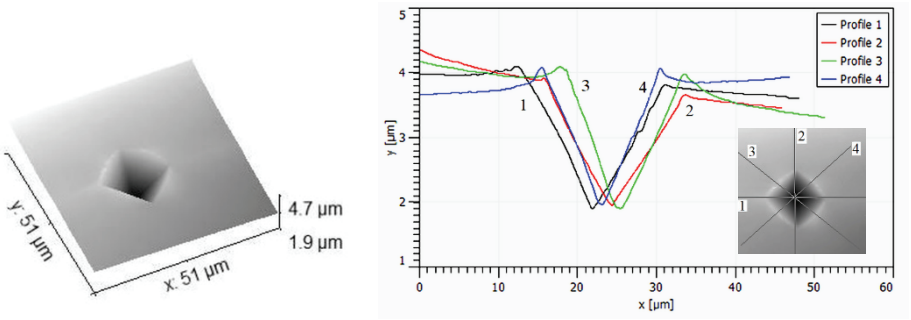



Fig. 2 – Microstructure of imprint made with a load of 500 mN on a $Pb_{1-x}Yb_xTe$/14 sample and its appearance in interference mode.




a b

Fig. 3 – (Color online) AFM. Surface microstructure near and inside the imprint applied to PbYbTe 99B02/4 crystal at a load of $P$ = 100 mN. a – 3D image of the imprint; b – profiles of the imprint. 2D view of the imprint and the layout of profiles 1–4 are shown in the lower right corner.

The microhardness measurement revealed a very weak dependence on the value of the applied load (Fig. 4). In general, the hardness tends to decrease with the indenter load increase. But at the smallest load (50 mN), a certain scatter in the value of hardness for different chips is detected. Whereas on chips 2, 4, 13 the hardness is close to each other, samples 6 and 11 showed higher values of $H$, and the hardness of sample 14 sharply decreased, which may be due to the inhomogeneity of the Yb distribution in the sample, which is more noticeable at low loads.

Therefore, it was of interest to consider the effect of the Yb concentration on the hardness of the samples under study. Since the Yb content changes nonmonotonically with an increase in cleavage number (Table 1), the microhardness value was presented in two versions: 1 – as a function of an increase in the sample number (Fig. 5) and 2 – as a function of an increase in the weight concentration of ytterbium (Fig. 6).

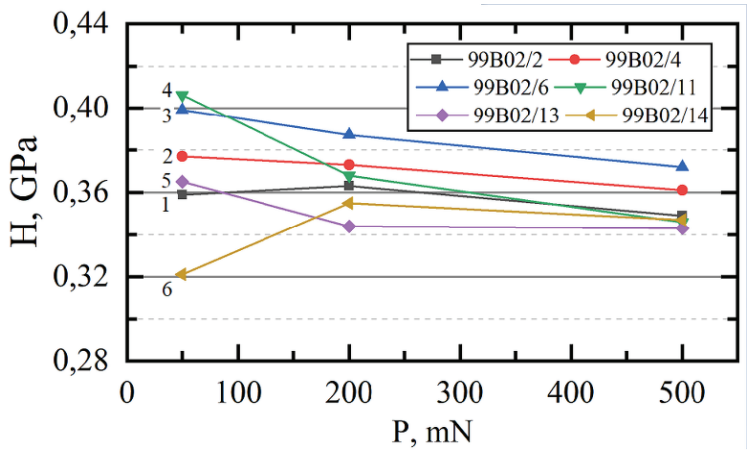



Fig. 4 – (Color online) $Pb_{1-x}Yb_xTe$ 99B02/. Microhardness as a function of applied load.

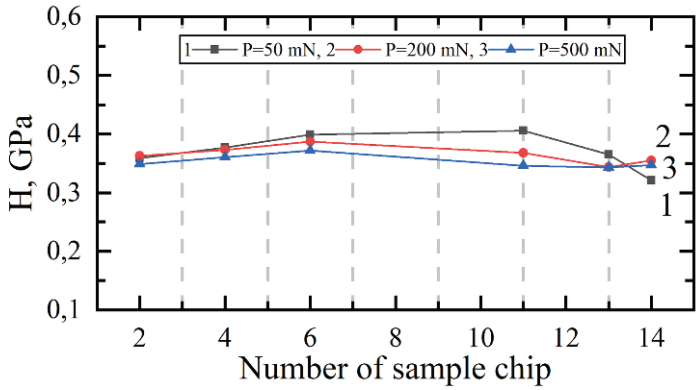



Fig. 5 – (Color online) $Pb_{1-x}Yb_xTe$. Microhardness as a function of sample piece number from the 99B02/ ingot.

As the presented results show, the hardness of lead telluride doped with ytterbium within the concentration range of (0.004 – 0.279) wt.%, both in the first and second cases, experiences a weak and nonmonotonic dependence on the Yb concentration, and these fluctuations occur within small limits of (0.032 – 0.042) GPa.

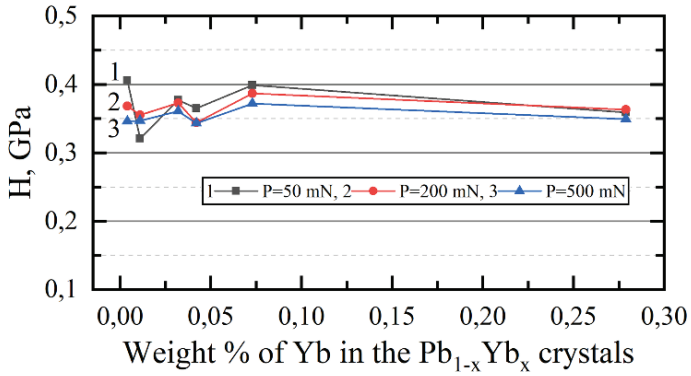



Fig. 6 – (Color online) Microhardness as a function of ytterbium content in crystals $Pb_{1-x}Yb_xTe$ 99B02/. *P*, mN: 1 – 50, 2 – 200, 3 – 500.

On the other hand, all these values are almost twice as less, than those of the hardness of pure undoped lead telluride ($H$ = 0.698 GPa) [9]. So, this result indicates that even such low Yb concentrations make a significant contribution to the change in the internal structure of lead telluride, being located in the places of Pb vacancies and leading to an increase in plasticity and a decrease in the microhardness of the latter.

### 3.2. ANISOTROPY OF THE SCLEROMETRIC MICROHARDNESS OF $Pb_{1-x}Yb_xTe$ CRYSTALS

In the previous section, we considered the characteristic features of the deformation of $Pb_{1-x}Yb_xTe$ crystals using the quasi-static deformation method. Another important way to identify the mechanical properties of materials is the sclerometric method or the indenter moving method, or otherwise the microscratching method. This method is valuable because it allows determining the anisotropy of the mechanical properties of materials, in particular, brittleness, plasticity, and the dependence of hardness on the crystallographic direction [13]. Usually, high anisotropic mechanical properties are manifested in crystals of low syngonies [14]. Considering that crystals $Pb_{1-x}Yb_xTe$ possess a cubic lattice of the NaCl type, it is of interest to determine what anisotropic properties of hardness are exhibited by these materials, which belong to the crystals of the highest system.

The tests were performed using one of the samples studied above, chip number 4. The results obtained using it are typical for other samples studied. As follows from Fig. 7, the $Pb_{1-x}Yb_xTe$ crystal exhibits low anisotropy of the sclerometric microhardness on the (001) plane, which is specified by these compounds belonging to the cubic system. The highest values of hardness are observed in the directions of the <100> type ($H_{s\ max}$ = 0.283 GPa), the lowest are along directions of movement of the <110> type ($H_{s\ min}$ = 0.205 GPa). Other of the measured

landmarks occupy intermediate positions (Table 2). The anisotropy coefficient is $k = H_{s[100]} / H_{s[110]} = 1.38$.

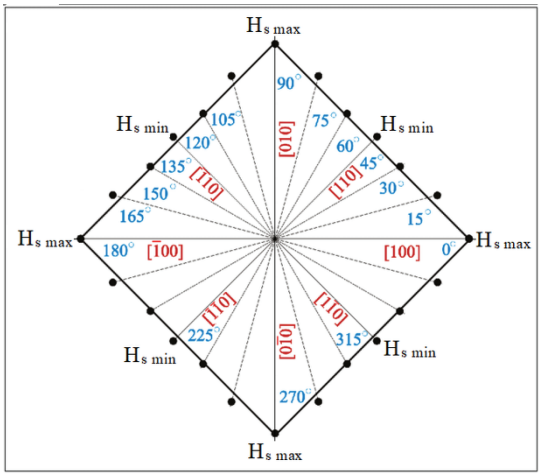



Fig. 7 – (Color online) Anisotropy of sclerometric hardness of crystal $Pb_{1-x}Yb_xTe$, sample 99B02/4.

*Table 2*

Microscratch hardness values within one quadrant

| Type | Location of micro-scratches | | | | | | |
|---|---|---|---|---|---|---|---|
| Angles, º | 0º | 15º | 30º | 45º | 60º | 75º | 90º |
| Hardness, GPa | 0.283 | 0.245 | 0.210 | 0.205 | 0.210 | 0.245 | 0.283 |
| Crystallographic direction | [100] | – | – | [110] | – | – | [001] |

The difference in the width of the scratches can also be revealed in Fig. 8. It can be seen that the scratches along [100] and [001] (0º and 90º) are narrower than the scratch along [110] (45º). The width of other four scratches occupies an intermediate position.

In addition, all scratches in Fig. 8 show another marked feature. The microstructure inside the scratches is not smooth, but intersected by thin lines-steps located perpendicular to the length of the scratches, *i.e.* perpendicular to the direction of the indenter movement. The question arises, what is the nature of these steps? The appearance of slip bands both inside and around scratches has been mentioned in many materials. Their appearance was explained by the activity of sliding elements characteristic of a particular crystal. So, for example, on crystals of antimonite ($Sb_2S_3$) at scratches of the [100] direction, plastic slip lines are located along the scratch. When changing the direction of scratching, they retain the same orientation [100], gradually becoming perpendicular to the scratch along [001] with the pronounced brittle fracture [14]. In the case of $Pb_{1-x}Yb_xTe$ crystals, the steps remain strictly perpendicular to the scratch at its different orientations

(see Fig. 8). Therefore, it seems that the appearance of such steps is of a different nature.

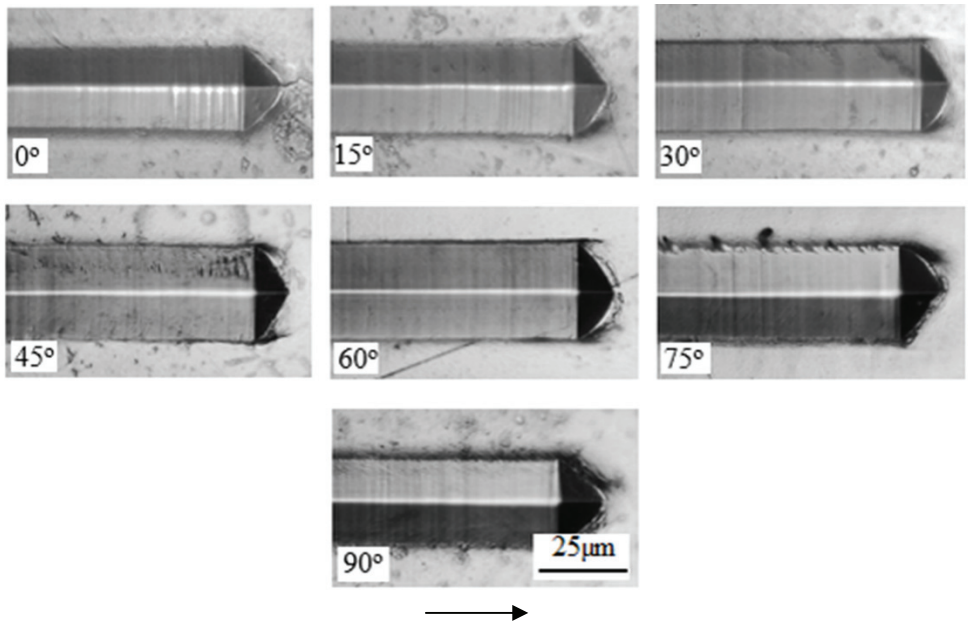



Fig. 8 – Crystal PbYbTe 99B02/4, plane (001). The shape of scratches applied along different crystallographic direction are: 0º and 90, which correspond to the directions [100] and [001], 45º – [110]. $P$ = 100 mN. The arrow shows the direction of the indenter movement.

To explain this effect, let us consider the features of the interaction of the indenter with the sample during the quasi-static indentation and during the indenter motion. It is known from the literature that under the action of a concentrated load, an inhomogeneous stress field arises in the material [13, 15]. As it deepens, the indenter encounters an increasing resistance from the sample. Ultrahigh compressive stresses occur under the indenter in the sample, which prevent the mass transfer into depth. When the pressure from the indenter becomes equal to the resistance from the sample, the indenter stops, and a plastic imprint of one or another size is formed in the material.

When scratching is applied, the stress distribution differs from that upon pressing. The scratch formation process consists of two stages: the formation of an imprint at the moment when the indenter touches the sample and its further elongation upon application of a pulling force with the scratch track formation. When the Vickers indenter moves “edge forward”, as in our case, its two edges are oriented in the direction of scratching, but at different angles: the front edge is at an acute angle, and the back edge is at an obtuse angle. The other two ribs are perpendicular to the direction of scratching. Therefore, in the Vickers imprints, the

projection of two edges is located along the scratch and forms the middle line of the track with the other two being perpendicular to the scratch (Fig. 9).

If we consider the morphology of scratches, we can state that the deformation steps in Fig. 9 are located exactly like those in Fig. 8 and represent the traces of the ribs of the indenter, which could arise as a result of the intermittent, jump-like movement of the indenter [16, 17]. The works are known, in which with the use of various materials, the uneven movement of two bodies relative to each other during their mutual sliding was revealed [18–20]. Here, the authors showed that the friction force between the surfaces of two bodies during sliding was not constant, but varied wavelike or jerkily. The specimen and indenter seem to "stick" to each other when a normal load is applied to the indenter until the elastic forces of the tangential load are sufficient for a jerk to start sliding.

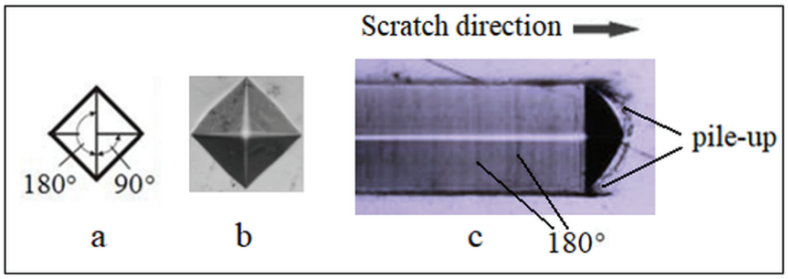



Fig. 9 – Diagram of evolution of formation of steps due to "edge forward" indenter motion.

If a scratch is formed by the sample plastic deformation, as in the case of lead telluride, then the plastic pile-ups are formed in front of and around the scratches, which provide additional resistance to the movement of the indenter. As an example, Fig. 10 shows a scratch applied to a PbYbTe 99B02/4 crystal at a load of $P$ = 100 mN. In 3D mode, Fig. 10a, pile-ups on the sides and in front of the scratch are clearly seen.

The evolution of surface relief as it approaches the scratch and inside it is shown in sections 1–6 (Fig. 10b) and in 2D mode (Fig. 10c). It can be seen that at some distance in front of the scratch there is a small pile-up (curve 1), which increases as the scratch is approached (curve 2). Curve 3 crosses the beginning of the scratch and a still higher pile-up, whose height remains approximately the same when crossing the zone of the scratch itself (curves 4–6).

Overcoming the resistance of the specimen during sliding, the elastic forces are decreased to a level below certain limits, and the indenter stops until the elastic forces are accumulated for the next jerk. In [20], under micromechanical deformations of styrene-acrylonitrile copolymer, it was shown that when a scratch is applied, the system fluctuates between two states: the state of energy accumulation, in which the indenter is almost stationary, and the slip state, in which the indenter moves.

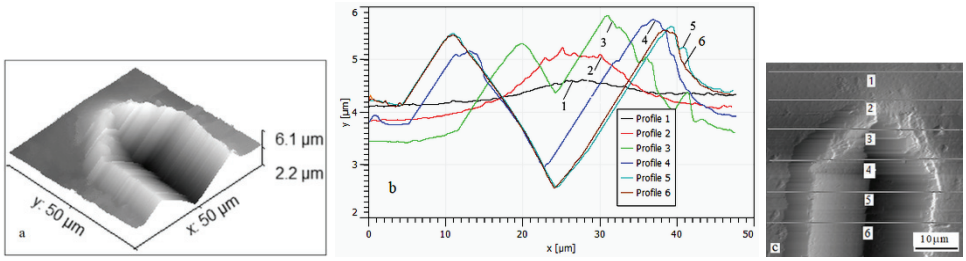



Fig. 10 – (Color online) AFM. Surface microstructure near and inside the scratch applied to PbYbTe 99B02/4 crystal at a load of $P$ = 100 mN; a – 3D image of the scratch; b – profiles 1–6, made as they approach the scratch and inside the scratch; c – 2D view of the scratch and the layout of profiles 1–6.

It can be concluded that a similar process takes place in our case as well, which results in the formation of the perpendicular deformation steps during microscratching of $Pb_{1-x}Yb_xTe$ crystals. Consequently, the perpendicular steps formation along the scratches on the crystals studied confirms the universal character of the jump-like mechanism of deformation of various materials during the indenter movement.

## 4. CONCLUSIONS

The study of the plastic deformation of $Pb_{1-x}Yb_xTe$ single crystals using the methods of quasi-static and sclerometric microindentation revealed a number of features characteristic of these crystals, as well as general patterns typical for various materials, determined by the specificity of the sclerometric method of indentation. A characteristic feature of $Pb_{1-x}Yb_xTe$ single crystals is their high plasticity and low microhardness. There are practically no pile-ups of displaced material around the imprints, which indicates the participation of the mechanism of compaction of the structure during plastic deformation, along with the usual dislocation mechanism of mass transfer during the formation of an imprint. It was revealed that $Pb_{1-x}Yb_xTe$ crystals have low hardness anisotropy along different crystallographic directions on the (001) plane, which is typical for cubic crystals. As a result of studying the morphology of scratches, the jump-like mechanism of the deformation process during the movement of the indenter was confirmed, which is common for poly- and single crystals of different types.

*Acknowledgements.* This work is supported financially by the National Agency for Research and Development of the Republic of Moldova under the grant no. 20.80009.5007.18.

The authors thank the researcher Lazar Dermenji, Laboratory of Materials for Photovoltaics and Photonics, IAPh, for the XRS-FP Analysis and to Dr. Tudor Braniste from the National Center for the Study of Materials and Testing of the Technical University of Moldova for measurements using AFM.

REFERENCES


1. K. Szamota-Sadowska, B.J. Kowalski, E. Guziewicz, *et al.*, *Influence of Yb on valence band density of states of CdYbTe and PbYbTe – a resonant photoemission study*. Acta Phys. Pol. A **90**(5), 943–946 (1996).
2. N. Abrikosov, L. Shalimova, *Semiconductor materials based on compounds $A^4B^6$*, Moscow: Science, 187 p. (1975). (in Rus.).
3. B. Askerov, *Electronic transport phenomena in semiconductors*, Moscow: Science, 320 p. (1985). (in Rus.).
4. N. A. Chernova, *Impurity states of ytterbium in alloys based on lead telluride* / Dissertation for the degree of candidate fiz.-mat. sciences. (in Rus.). http://www.disser-cat.com/content/primesnye-sostoyaniya-itterbiya-v-splavakh-na-osnove-tellurida-svintsa
5. B.A. Volkov, L.I. Ryabova, D.R. Khokhlov, *Impurities with variable valence in solid solutions based on lead telluride*, Advances in Phys. Sci. **172**(8), 875–906 (2002). (in Rus.).
6. V. Nicorici, D. Grabco, Z. Barbos, M. Popa, C. Burlacu, *Micromechanical properties of the $Pb_{1-X}Yb_XTe$ ternary semiconductors*, Book of abstracts MSCMP, 163 (2018).
7. D. Grabco, Z. Barbos, M. Popa, V. Nikorici, *Electrophysical properties of crystals $Pb_{1-x}Yb_xTe$*. Proceedings of Conf. *Integration through research and innovation*, 286–288 (2018). (in Rus.).
8. D. Z. Grabco, V. Z. Nicorici, Z. A. Barbos, D. Topal, O. A. Shikimaka, *Micromechanical Properties and Plastic Deformation Features of the $Pb_{1-x}Yb_xTe$ Ternary Semiconductors*. In: 4th International Conference on Nanotechnologies and Biomedical Engineering. Proceedings of ICNBME-2019, September 18–21, 2019, Chisinau, Moldova, IFMBE Proceedings, Springer, 149–153 (2019). https://doi.org/10.1007/978-3-030-31866-6
9. N.N. Kolesnikov, E.B. Borisenko, S.A. Shevchenko, A.V. Timonina, D.N. Borisenko, B.A. Gnesin, *Mechanical and electrical properties of PbTe ceramics*, Deformation and destruction of materials, **6**, 31–39, (2010). (in Rus.).
10. Yu.S. Boyarskaya, I.I. Melent'ev, D.Z. Grabco, *On the nature of hardness anisotropy on the (001) face of PbS and CaF2 single crystals*, Physics **2**, 84–88 (1971). (in Rus.).
11. V. Beshliu, L. Lungu, A. Nicorici, V. Nicorici, *Yb impurity influence on parameters of PbTe crystals grown from the melt.* Proceedings of International Semiconductor Conference, Sinaia (Romania), **1**, 131–134 (2000). (https://www.tib.eu/en/search/id/ieee:doi~10.1109%252FSMICND.2000.890203/Yb-impurity-influence-on-parameters-of-PbTe-crystals?cHash=a98c57ac52fc262e4df49056597bc565)
12. V.K. Grigorovich, *Hardness and microhardness of metals*, Moscow: Nauka, 232 p. (1976). (in Rus.).
13. Yu.S. Boyarskaya, D.Z. Grabco, M.S. Kats, *Physics of microindentation processes*, Chisinau, Shtiintsa, 294 p. (1986). (in Rus.).
14. Yu.S. Boyarskaya, *Microhardness of crystals during microhardness tests*, Chisinau, Shtiintsa, 235 p. (1972). (in Rus.).
15. W. Prager, Ph.G. Hodge, *Theory of Perfectly Plastic Solids*, New York – John Wiley and Sons, London – Chapman and Hall, 398 p. (1963).
16. O. Shikimaka, A. Prisacaru, *Deformation mechanisms under nanoscratching of Si: effect of scratching speed, load and indenter orientation*, Mater. Res. Express **6**, 085011 (2019). https://doi.org/10.1088/2053-1591/ab1a0d.
17. D. Grabco, O. Shikimaka, C. Pyrtsac, Z. Barbos, M. Popa, A. Prisacaru, D. Vilotic, M. Vilotic, S. Alexandrov, *Microstructures Generated in AISI 316L Stainless Steel by Vickers and Berkovich Indentations*, Mat. Sci. Eng. A **805 C**, 140597 (2021). https://doi.org/10.1016/j.msea.2020.140597.
18. F. P. Bowden, L. Leben, *The nature of sliding and the analysis of friction*, Proc. R. Soc. London A, **169**, 371–391 (1939). https://doi.org/10.1098/rspa.1939.0004.
19. F.P. Bowden, D. Tabor, *The Friction and Lubrication of Solids*, Part I, Clarendon Press, Oxford, 424 p. (1950).
20. K. Li, B.Y. Ni, J.C.M. Li, *Stick-slip in the scratching of styrene-acrylonitrile copolymer*, J. Mater. Res., **11**(6) (1996), 1574–1580. doi: https://doi.org/10.1557/JMR.1996.0197.